19

Synthesis, crystal structure and thermodynamic properties of apatite $Pb_3Bi_2(GeO_4)_3$

© L.T. Denisova[1], M.S. Molokeev[1,2], E.O. Golubeva[1], N.V. Belousova[1], V.M. Denisov[1]

[1] Siberian Federal University,
Krasnoyarsk, Russia
[2] Kirensky Institute of Physics, Federal Research Center KSC SB, Russian Academy of Sciences,
Krasnoyarsk, Russia

E-mail: ldenisova@sfu-kras.ru

Received March 13, 2022
Revised March 13, 2022
Accepted March 15, 2022

Apatite $Pb_3Bi_2(GeO_4)_3$ was obtained by the solid-phase method from the initial oxides of PbO, Bi_2O_3 and GeO_2 by sequential firing in air at temperatures of 773−1003 K. Its crystal structure has been refined by X-ray diffraction. The high-temperature heat capacity (350−1000 K) of this compound was measured by differential scanning calorimetry. Based on these data, the main thermodynamic functions are calculated. Keywords: apatite bismuth-lead germanate, solid-phase synthesis, high-temperature heat capacity, thermodynamic properties

Keywords: apatite bismuth-lead germanate, solid-phase synthesis, high-temperature heat capacity, thermodynamic properties.

DOI: 10.21883/PSS.2022.07.54599.312

1. Introduction

In recent years, there has been a steady interest in compounds with the apatite structure $M_{10}(ZO_4)_6X_2$ ($M = Na^+$, K^+, Ca^{2+}, Sr^{2+}, Pb^{2+}, La^{3+}, Eu^{3+}, Bi^{3+} etc.; $Z = Ge^{4+}$, Si^{4+}, V^{5+} etc.; $X = F^-$, Cl^-, Br^-, O^{2-} etc.) [1–8]. This is due to the wide possibilities of practical application as biocompatible ceramics, laser, fluorescent and acoustic-optical materials, luminophores, catalysts [9–13]. Compounds of this type crystallize in a hexagonal lattice (space group $P6_3/m$) and have the ability to replace their structural units with other ions in a wide range of element proportions without significant structural distortion [14]. The latter allows for obtaining new functional materials. For example, replacing lead in apatite $Pb_5(GeO_4)(VO_4)_2$ with rare earth elements enabled to obtain $Pb_{10-x}R_x(GeO_4)_{2+x}(VO_4)_{4-x}$ (R = La, $x = 2$ [15]; R = Pr, $x = 2$ [6], $x = 0-3$ [16]; R = Nd, $x = 0-3$ [6]) and with bismuth — $Pb_{10-x}Bi_x(GeO_4)_{2+x}(VO_4)_{4-x}$ ($x = 0-3$) [17]. It should be noted that in $Pb_{10-x}R_x(GeO_4)_{2+x}(VO_4)_{4-x}$ or in $Pb_{10-x}Bi_x(GeO_4)_{2+x}(VO_4)_{4-x}$ compounds maximum value is $x = 3$. In case of $x = 4$ we obtain the compound $Pb_3Bi_2(GeO_4)_3$. When studying glasses of the $PbO-Bi_2O_3-GeO_2$ system, the presence of a phase with the presumed composition $Pb_3Bi_2Ge_3O_{12}$, which is similar to the garnet formula, is found [18]. However, its non-isotropic behavior in polarized light excludes the garnet-like arrangement of isolated GeO_4 tetrahedra. The authors of the article [19], who studied this system, also noted the presence of $Pb_3Bi_2(GeO_4)_3$. By homogenization of $3PbO \cdot Bi_2O_3 \cdot 3GeO_2$ melt in a platinum crucible at 1100 K and subsequent cooling at a rate of 5 K/h and spontaneous crystallization the $Pb_3Bi_2(GeO_4)_3$ single crystals were obtained [20]. Transparent slightly brown single crystals had an apatite structure. Their crystal structure was determined (sp. gr. $P6_3/m$). These results were updated later [21]. $Pb_3Bi_2(GeO_4)_3$ single crystals were grown in a similar way [20], but a gold crucible was used instead of a platinum crucible. During the growth of crystals from the melt, a part of the Pt crucible dissolves, which leads to the appearance of brownish inclusions. This was not observed when using Au crucibles. Both single crystals and powders were used to describe the crystal structure. In this case, the crystal structure is described by sp. gr. $P6_3$ with lattice cell parameter values $a = 10.0182(7)$ Å, $c = 7.2612(7)$ Å. A review of structural deviations and crystal chemistry of apatites was made by the authors of the article [22]. Symmetry reduction ($P6_3/m \rightarrow P6 \rightarrow P6_3 \rightarrow P3 \rightarrow P2_1/m \rightarrow P2_1$) is considered in articles [21–23].

The purpose of this article is the synthesis, study of the crystal structure and thermodynamic properties of $Pb_3Bi_2(GeO_4)_3$ apatite.

2. Sample synthesis and experimental technique

The $Pb_3Bi_2(GeO_4)_3$ compound was obtained by solid-phase synthesis from the initial oxides PbO, Bi_2O_3 — extra-pure grade, GeO_2 — 99.999%. A stoichiometric mixture of pre-calcined oxides was ground in an agate mortar and pressed into tablets. They were sequentially burned in air at 773 and 873 K (by 10 h), 3 times at 973 K (for 30 h) and 1003 K (10 h). To achieve the completeness of the solid-phase reaction, the tablets were ground and pressed again

every 10 h. The phase composition of the obtained samples was controlled using X-ray diffraction analysis on an X'Pert Pro MPD diffractometer (PANalytical, the Netherlands) using CuK_α radiation. Diffraction patterns were recorded at room temperature with a high-speed PIXcel detector in the angular interval $2\theta = 10-100°$ with a step of 0.013°. Exposure time per step is 2 s. The Rietveld refinement was carried out in the TOPAS 4.2 [24] program. It has been established that the synthesized compound $Pb_3Bi_2(GeO_4)_3$ contains approximately 1% of impurities in the form of $Bi_4Ge_3O_{12}$. The obtained apatite had light yellow color.

The heat capacity of $Pb_3Bi_2(GeO_4)_3$ was measured on an STA 449 C Jupiter thermal analyzer (NETZSCH, Germany) by differential scanning calorimetry in air. The experimental technique is similar to that described in the articles [25,26]. The error in heat capacity measurements did not exceed 2%.

3. Experimental results

All reflections were indexed by a hexagonal cell (sp. gr. $P6_3/m$) with parameters close to $Pb_5(GeO_4)(VO_4)_2$ [27]. Therefore, the structure of this crystal was taken as a starting model for refinement. To transform the structure, Pb/Bi ions were placed in both independent positions of lead ions (Pb1 and Pb2). Their position occupancies were refined taking into account the fact that the sum of the occupancies in each of the positions is equal to 1. As a result, it turned out that the Pb1 position is 100% occupied by Bi ions, and Pb2 position is 100% occupied by Pb ions (Fig. 1). The only Ge/V position was 100% occupied by Ge ions. The thermal parameters of all atoms were refined in the isotropic approximation. Refinement proceeded stably and gave low values of R-factors (Table 1, Fig. 2). Atomic coordinates and main bond lengths are provided in Tables 2 and 3, respectively.

We have previously shown that replacement of lead with bismuth in $Pb_{10-x}Bi_x(GeO_4)_{2+x}(VO_4)_{4-x}$ apatite (change x from 0 to 3) leads to a decrease in lattice cell parameters a, c and V and an increase in density d [17]. From Fig. 3 it follows that with an increase in x up to 4 this trend

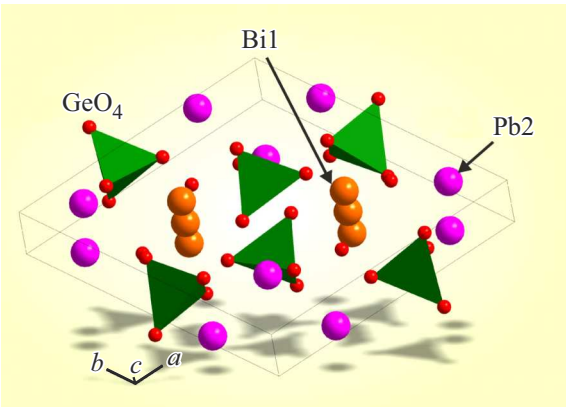

Figure 1. Crystal structure of $Pb_3Bi_2(GeO_4)_3$.

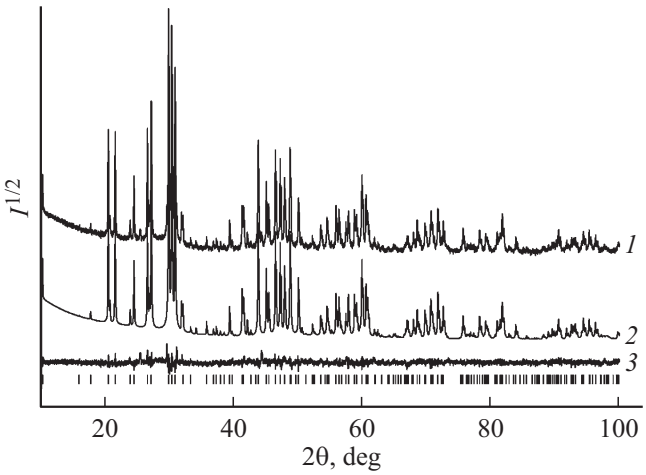

Figure 2. Experimental (*1*), calculated (*2*) and difference (*3*) X-ray profiles of $Pb_3Bi_2(GeO_4)_3$ after clarifications by the derivative difference minimizing method; strokes are calculated positions of reflections.

is preserved (the values of the lattice cell parameters of apatites with x values equal to 0, 1, 2 and 3 are taken from the article [17]).

Since there is no information on the thermal stability of apatite $Pb_3Bi_2(GeO_4)_3$ in the literature, differential thermal

Table 1. Basic shooting parameters and refinement of the crystal $Pb_3Bi_2(GeO_4)_3$

Parameters	this article	[20]
Sp. gr.	$P6_3/m$	$P6_3/m$
a, Å	10.04987(11)	10.034(1)
c, Å	7.29076(9)	7.267(2)
V, Å^3	637.711(16)	633.60
Z	2	2
2θ-interval, °	10–100	–
R_{wp}, %	8.82	–
R_p, %	6.49	–
R_{exp}, %	4.93	–
R_B, %	1.99	–
χ^2	1.79	–

Note. a, c are cell parameters; V is cell volume; uncertainty factors: R_{wp} is weight profile, R_p is profile, R_{exp} is expected, R_B is integral; χ^2 is quality of fit.

Table 2. Atomic coordinates and isotropic thermal parameters of the $Pb_3Bi_2(GeO_4)_3$ crystal

Atom	x	Y	z	B_{iso}, Å^2	Occupancy
Bi1	1/3	2.3	0.0103(5)	3.42(11)	1.0(3)
Pb2	0.25618(19)	0.0031(3)	0.25	2.44(12)	1.0(3)
Ge	0.3983(5)	0.3854(6)	0.25	2.21(15)	1
O1	0.309(3)	0.4095(3)	0.25	6.6(5)	1
O2	0.602(3)	0.505(2)	0.25	6.6.(5)	1
O3	0.3490(18)	0.2628(18)	0.064(2)	6.6(5)	1

Table 3. Principal bond lengths in $Pb_3Bi_2(GeO_4)_3$

Bond	Bond length, Å	Bond	Bond length, Å
Bi1–O1	2.381(17)	Pb2–O3	2.662(15)
Bi1–O2^{i}	2.850(15)	Pb2–O3^{v}	2.472(15)
Bi1–O3^{ii}	2.954(15)	Ge–O1	1.734(19)
Pb2–O1^{iii}	2.85(3)	Ge–O2	1.78(2)
Pb2–O2^{iv}	2.09(2)	Ge–O3	1.730(15)

Note. Elements of symmetry: (i) $-x+1, -y+1, z-1/2$; (ii) $y, -x+y+1, -z$; (iii) $-x+y, -x, -z+1/2$; (iv) $-y+1, x-y, -z+1/2$; (v) $y, -x+y, -z$.

analysis (DTA — differential scanning calorimetry, DSC) was carried out. The experiments were carried out on the same thermal analyzer, only with other holders. The DTA data are shown in Fig. 4. It can be seen that in the studied temperature range there is only one endo effect, the maximum of which is 1019 K, and its area is 84.8 J/g.

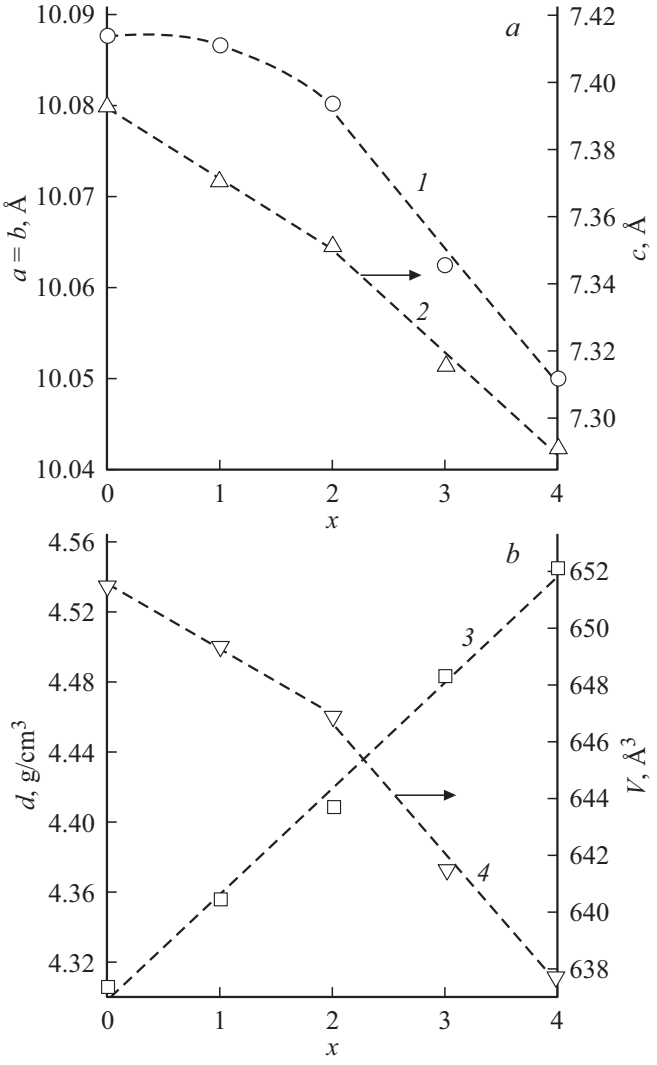

Figure 3. Effect of bismuth substitution on the crystallographic parameters of the lattice$Pb_{10-x}Bi_x(GeO_4)_{2+x}(VO_4)_{4-x}$ ($x = 0-4$).

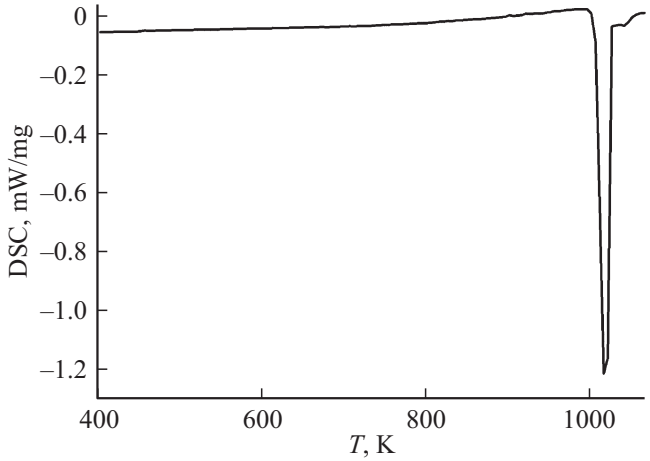

Figure 4. DTA curve of apatite $Pb_3Bi_2(GeO_4)_3$.

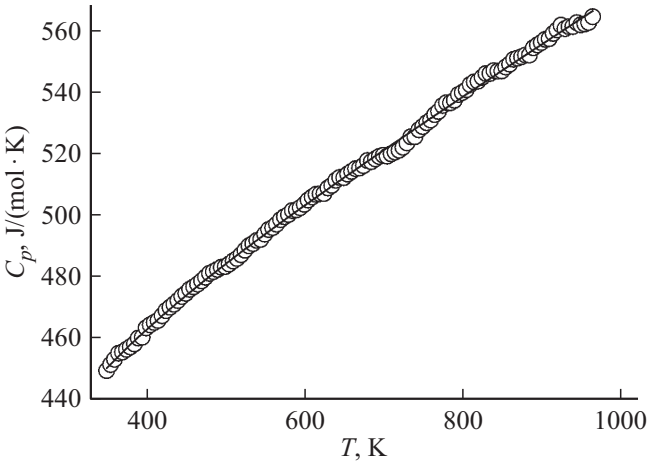

Figure 5. Effect of temperature on molar heat capacity $Pb_3Bi_2(GeO_4)_3$.

Figure 5 shows the effect of temperature on the molar heat capacity C_p for $Pb_3Bi_2(GeO_4)_3$. In the region 350–1000 K, the values C_p naturally increase, and there are no extrema on the dependence $C_p = f(T)$. This, together with the DTA data (Fig. 4), allows us to consider that $Pb_3Bi_2(GeO_4)_3$ apatite does not have polymorphic transformations in this temperature range. It has been established that the experimental data on the heat capacity of the studied apatite are well described by the Mayer–Kelly equation [28]:

$$C_p = a + bT - cT^{-2}, \quad (1)$$

which has the following form for $Pb_3Bi_2(GeO_4)_3$ ($J \cdot K^{-1} \cdot mol^{-1}$):

$$C_p = (411.20 \pm 1.52) + (163.5 \pm 1.6) \cdot 10^{-3}T - (22.25 \pm 1.58) \cdot 10^{5}T^{-2}. \quad (2)$$

The correlation coefficient for equation (2) is 0.9993, and the maximum deviation of the experimental points from the

Table 4. Thermodynamic properties $Pb_3Bi_2(GeO_4)_3$

T, K	C_p, $J \cdot K^{-1} \cdot mol^{-1}$	$H(T)-H(350\,K)$, $kJ \cdot mol^{-1}$	$S(T)-S(350\,K)$, $J \cdot K^{-1} \cdot mol^{-1}$	$\Delta G/T^*$, $J \cdot K^{-1} \cdot mol^{-1}$
350	450.2	–	–	–
400	462.7	22.83	60.95	3.87
450	473.8	46.25	116.1	13.32
500	484.0	70.19	166.6	26.22
550	493.8	94.64	213.1	41.03
600	503.1	119.6	256.5	57.23
650	512.2	144.9	297.1	74.18
700	521.1	170.8	335.4	91.40
750	529.9	197.1	371.7	108.9
800	538.5	223.8	406.2	126.5
850	474.1	250.9	439.1	143.9
900	555.6	278.5	470.6	161.2
950	573.5	338.3	533.4	197.1
1000	575.8	346.4	541.4	201.8

Note. * $-\Delta G/T^* = [H(T)-H(350\,K)]/T-[S(T)-S(350\,K)]$.

smoothing curve is 1.2%. Using equation (2), the main thermodynamic functions of $Pb_3Bi_2(GeO_4)_3$ are calculated based on the known thermodynamic relations. These results are given in Table 4. It was not possible to compare our results on the heat capacity of this apatite with the data of other authors due to their absence. Therefore, we will make such a comparison with the calculated values by the method of group contributions, which is based on the use of the equation

$$C_p = a + bT + cT^{-2} + dT^2, \qquad (3)$$

which parameters are determined on the basis of the tables given in the article [29]. Note that the main advantage of the group contributions method is that it does not require any additional information about the analyzed compound. We have established that at 298 K the calculation gives the value of C_p by 2.4% less than that obtained by equation (2). However, this method describes the temperature dependence $C_p = f(T)$ poorly. Starting from $T = 400$ K, the calculated values exceed the experimental values C_p (the higher the temperature, the greater this difference; this is not shown in the figure). The analysis of the group contributions method made by the authors of the article [30] showed that it gives satisfactory results for C_p at 298 K, while at other temperatures differences with experimental results can be observed. The latter was also noted by the authors of this method [29].

4. Conclusion

$Pb_3Bi_2(GeO_4)_3$ apatite was synthesized by burning of stoichiometric mixtures of PbO, Bi_2O_3, and GeO_2 in air at temperatures 773–1003 K. The effect of temperature on its molar heat capacity is studied. It was found that in the temperature range 350–1000 K the temperature dependences $C_p = f(T)$ are well described by the Mayer–Kelly equation. On the basis of experimental data, the thermodynamic properties of apatite are calculated.

Acknowledgments

The authors express their gratitude to the Krasnoyarsk Regional Resource Sharing Center of the Federal Research Center „Krasnoyarsk Research Center“ of the Siberian Branch of the Russian Academy of Sciences.

Funding

This work was partially supported within the scope of the state assignment for science of FSAEI HE „Siberian Federal University“, project number FSRZ-2020-0013.

Conflict of interest

The authors declare that they have no conflict of interest.

References

[1] E.I. Get'man, N.V. Yablochkova, S.N. Loboda, V.V. Prisedsky, V.P. Antonovich, N.A. Chivireva. J. Solid State Chem. **181**, *9*, 2386 (2008).
[2] E. Chakroun-Ouadhour, R. Ternane, D. Ben Hassen-Chehimi, M. Trabelsi-Ayadi. Mater. Res. Bull. **43**, *8–9*, 2451 (2008).
[3] P. Ptáček, T. Opravil, F. Šoukal, E. Bartoničková, J. Tkacz. Ceram. Int. **43**, *10*, 7827 (2017).
[4] M. Pasero, A.R. Kampf, C. Ferraris, I.V. Pekov, J. Rakovan, T.J. White. Eur. J. Mineral. **22**, *2*, 163 (2010).
[5] T. Baikie, S.S. Pramana, C. Ferraris, Y. Huang, E. Kendrik, K.S. Knight, Z. Ahmad, T.J. White. Acta Cryst. **B66**, *1*, 1 (2010).
[6] N.V. Yablochkova. ZhNKh **58**, *7*, 871 (2013) (in Russian).
[7] E.N. Bulanov, K.S. Korshak, M.I. Lelet, A.V. Knyazev, T. Baikie. J. Chem. Thermodyn. **124**, 74 (2018).

[8] L.T. Denisova, E.O. Golubeva, N.V. Belousova, V.M. Denisov, N.A. Galiakhmetova. FTT **61**, *7*, 1397 (2019) (in Russian).
[9] T. Kanazawa. Neorganicheskiye fosfatnyye materialy. Nauk. dumka, Kiev (1998). 298 p. (in Russian).
[10] Yu. Zang, Sh. Tan, Ya Yin. Ceram. Int. **29**, 113 (2003).
[11] D. Grossin, S. Rollin-Martinez, C. Estournus, F. Rossignol, E. Champion, C. Comdes, C. Rey, C. Geoffroy, C. Drouet. Acta Biomater. **6**, *2*, 577 (2010).
[12] J. Zhang, H. Liang, H. Yu, Q. Su. Mater. Chem. Phys. **114**, *1*, 242 (2009).
[13] L. Kovács, Á. Péter, M. Gospodinov, R. Capelletti. Phys. Status Solidi C **2**, *1*, 689 (2005).
[14] Sh.Yu. Azimov, A.A. Ismatov, N.F. Fedorov. Apatity i ikh redkozemel'nyye analogi. FAN, Tashkent (1990). 116 p. (in Russian).
[15] V.D. Zhuravlev, Yu.A. Velikodny. V.D. Zhuravlev, Yu.A. Velikodny. ZhNKh **54**, *10*, 1626 (2009) (in Russian).
[16] L.T. Denisova, Yu.F. Kargin, E.O. Golubeva, G.M. Zeer, A.K. Abkaryan, V.M. Denisov. Neorgan. materialy **56**, *10*, 1081 (2020) (in Russian).
[17] L.T. Denisova, M.S. Molokeev, V.M. Denisov, E.O. Golubeva, N.A. Galiakhmetova. FTT **62**, *11*, 1828 (2020) (in Russian).
[18] E.F. Riebling. Mater. Res. Bull. **10**, *1*, 23 (1975).
[19] A. Munpakdee, K. Pengpat, T. Tunkasiri, D. Holland. Adv. Mater. Res. **55**–**57**, 473 (2008).
[20] H.H. Otto, W. Müller-Lierhelm. J. Appl. Cryst. **11**, 158 (1978).
[21] H.H. Otto. Cryst. Res. Technol. **50**, *12*, 922 (2015).
[22] T.J. White, D. Zhili. Acta Cryst. B **59**, *1*, 1 (2003).
[23] T.J. White, C. Ferraris, J. Kim, M. Srinivasan. Rev. Mineral. Geochem. **57**, 307 (2005).
[24] Bruker AXS TOPAS V4: General profile and structure analysis software for powder diffraction data. — User's Manual. Bruker AXS, Karlsruhe, Germany (2008).
[25] L.T. Denisova, L.A. Irtyugo, Yu.F. Kargin, V.V. Beletsky, V.M. Denisov. Neorgan. materialy **53**, *1*, 71 (2017) (in Russian).
[26] V.M. Denisov, L.T. Denisova, L.A. Irtyugo, V.S. Biront. FTT **52**, *7*, 1274 (2010) (in Russian).
[27] S.A. Ivanov. ZhSKh **31**, *4*, 80 (1990) (in Russian).
[28] C.G. Maier, K.K. Kelley. J. Am. Chem. Soc. **54**, *8*, 3243 (1932).
[29] A.T.M.G. Mostafa, J.M. Eakman, M.M. Montoya, S.L. Yarbro. Ind. Eng. Chem. Res. **35**, *1*, 343 (1996).
[30] J. Leitner, D. Sedmidubský, P. Chuchvalec. Geramics-Silikáty **46**, *1*, 29 (2002).